The Hall-Petch effect as a manifestation of the general size effect

Y. Li,[a] A.J. Bushby[b] and D.J. Dunstan[a*]

[a] School of Physics and Astronomy,
[b] School of Engineering and Materials Science,
Queen Mary University of London,
London E1 4NS, England.

The experimental evidence for the Hall-Petch dependence of strength on the inverse square-root of grain size is reviewed critically. Both the classic data and more recent results are considered. While the data are traditionally fitted to the inverse square-root dependence, they also fit well to many other functions, both power-law and non-power-law. There have been difficulties, recognised for half-a-century, in the inverse square-root expression. It is now explained as an artefact of faulty data analysis. A Bayesian meta-analysis shows that the data strongly supports the simple inverse or lnd/d expressions. Since these expressions derive from underlying theory, they are also more readily explicable. It is concluded that the Hall-Petch effect is not to be explained by the variety of theories found in the literature, but is a manifestation of, or underlain by, the general size effect observed throughout micromechanics, due to the inverse relationship between the stress required and the space available for dislocation sources to operate.

Short title
Hall-Petch effect as the general size effect

Keywords
Dislocations; Grain boundaries; Elastic-plastic material; Probability and statistics; Hall-Petch equation.

* Corresponding author, E-mail d.dunstan@qmul.ac.uk

1. Introduction

In the years around 1950, two effects of size were identified in the strength of materials; both can be summarised as *smaller is stronger*. Hall [1] and Petch [2] found that the strength of iron and steel increases when the grain size is smaller. On the basis of the theoretical work on dislocation pile-up by Eshelby *et al.* [3], their work established experimentally the eponymous relationship,

$$\sigma(d) = \sigma_0 + \frac{k_{HP}}{\sqrt{d}} \tag{1}$$

where d is the grain size, $\sigma(d)$ is the stress at yield or a flow stress at higher plastic strains, σ_0 is the corresponding stress for large single crystals or very large-grained material (we refer to it here as the bulk stress), and k_{HP} is a constant that may be predicted by theory or may be considered to be a material constant. This relationship was soon reported to apply quite generally to other metals, however, we show here quantitatively that the data does not in fact support Eq.1.

On the other hand, Frank and van der Merwe [4] and later van der Merwe and co-workers, and especially Matthews and his co-workers, investigated theoretically and experimentally the elastic misfit strain that could be supported by thin epitaxial layers of one metal or semiconductor grown on another. By considering the force balance on threading dislocations or the minimum energy configuration of the system, Matthews developed the relationship between the maximum or critical thickness h_c for a given misfit ε_0 [5]. For an 001-oriented layer this is given as

$$h_c = \frac{b(1-\nu\cos^2\theta)}{8\pi\varepsilon_0(1+\nu)\cos\lambda}\ln\frac{h_c}{b} \tag{2}$$

where b is the magnitude of the Burgers vector, ν is the Poisson's ratio, and θ and λ are angles between the slip plane and the Burgers vector and the growth plane. Many versions of Eq.2 were given subsequently by various authors [6].

Over the decades that followed, these two size effects were addressed by different communities, with very little interaction. Matthew's critical thickness theory was developed and applied within, largely, the semiconductor device community in the context of the strained heterostructures required for, e.g., semiconductor lasers [7] and high-electron-mobility transistors [8]. This theory remains essentially correct. The principal modification relevant here was the realisation that for significant plastic relaxation of the elastic strain a relaxation critical thickness needed to be defined, about four or five times the h_c of Eq.2, to take account of the operation of dislocation sources [9-11, 6]. From Eq.2, elastic strain rather than stress (i.e. stress normalised by the relevant elastic modulus), and normalised size (d measured in units of Burgers vector b or lattice constant a_0), are the relevant parameters. These considerations lead to a general size-dependence equation,

$$\varepsilon_{el}(d) = \varepsilon_0 + \frac{k\ln d}{d} \tag{3}$$

where the dimensionless constant k is expected to be of the order of unity. In the present paper d will the grain size in units of a_0 and the bulk strength is described by the elastic strain $\varepsilon_0 = \sigma_0 / Y$. Eq.3 is theoretically applicable to any situation where a dimension (such as grain size) constrains the size of the dislocation sources that have to operate if

plasticity is to occur, and their dislocation curvatures. We refer to it below as the size-effect equation from dislocation curvature (the EDC equation). Our Bayesian meta-analysis of a large body of Hall-Petch data in Section 3 below shows that this equation is supported by the data.

Meanwhile, in the wider materials science community, a number of theories were put forward to supplement the pile-up theory [4] in accounting for the inverse-square root of d in Eq.1 (see Section 4). Size effects became recognised in micro-mechanical testing generally, in nano-indentation [12], in thin wires under torsion [13], in thin foils in flexure [14], and most dramatically in micropillars under compression [15]. Despite a few key papers – such as that of Nix [16] applying critical thickness theory to thin films, that of Thompson [17] addressing grain-size effects in thin films in the framework of critical thickness theory, and our own [18] applying critical thickness theory to wire torsion and foil bending – theories of the micromechanical size effect proliferated in parallel with the various theories of the Hall-Petch effect. One symptom of this was the expression of the effect of the size of the specimen or of the loaded region in micromechanical testing as

$$\sigma(a) = \sigma_0 + ka^{-x} \qquad (4)$$

where a is some suitable characteristic dimension such as micropillar diameter or indentation contact radius. Much effort has been invested in finding appropriate values of the scaling exponent x for particular datasets, particular materials, for types of materials such as FCC or BCC metals, and for large collections of data (e.g. [19, 20]. However, we have suggested that such efforts are in vain. Despite apparent good fits to Eq.4 with various x in the range $0 < x < 1$, we proposed that $x = 1$ (or the Eq.3 $\ln d / d$) is better supported by the data [21].

Returning to the Hall-Petch effect, many authors have considered exponents other than $x = ½$. Some proposed other exponents because they fit some datasets (e.g. $x = ¼$ [22], $x = 0.66$ [23]). Baldwin [24] and Kocks [25, 26] pointed out the difficulty (or impossibility) of deciding which exponent fits the data best. On theoretical grounds closely related to the Matthews theory of Eq.2, Bragg, as early as 1942 [27], and Kocks [26] proposed $x = 1$. Hirth acknowledged these earlier proposals, but did not consider them further and adopted $x = ½$ [28]. Narutani and Takamura [29] showed data for large-grain nickel fitting better $x = 1$ at high strain. More recently, Arzt [30] and Saada [31] recognised the theoretical arguments for $x = 1$ but also the strength of the experimental evidence for $x = ½$.

Until recently, it is only in the context of the relationship between subgrain or dislocation cell size and stress during work-hardening that $x = 1$ has been considered seriously both experimentally [32-34] and theoretically [35-38]. Following Matthews [5], the argument of similitude notes that if a dislocation structure is at equilibrium under a stress τ, then if that structure is rescaled to a size n times smaller, the stress must now be $n\tau$. Raj and Pharr [34] collated a large amount of experimental data and identified a correlation between the prefactor and the exponent, a correlation of the type that suggests that the range of fitting parameters is simply due to experimental error (see [39, 40]. It may be thought surprising none of these authors considered extending the argument from sub-grains to the Hall-Petch grain-size effect too.

Recently, there has renewed interest in data, simulation and theory suggesting $x > ½$ for the Hall-Petch effect itself [41-44]. More typically, Hansen [45] concludes that

although no mechanism has been quantified to the extent that it would verify Eq.1, nevertheless Eq.1 is empirical and has predictive capability. Indeed, Hahn and Meyers [44] note that Eq.1, $x = ½$, with the associated theory of pile-up, is so deeply embedded in the fabric of materials science as to be indelible.

In a previous paper we showed that the micromechanical data is consistent with Eq.4 with $x = 1$, and with Eq.3 with $k \sim 1$. We drew attention to the complete lack of any data falling *under* the line of Eq.3 with $k \sim 1$ and $\varepsilon_0 = 0$, implying that Eq.3 thus describes the *minimum* strength, due to the size effect [21]. Then other strengthening mechanisms lead to data above the line, but if plasticity occurs through dislocation multiplication and motion, there are no weakening mechanisms to give data below the line. A collection of datasets from the literature displaying the Hall-Petch effect are likewise concentrated above this line. We proposed that this can be taken as experimental *support* for the applicability of Eq.3 to the Hall-Petch effect, while the data are merely *consistent* with Eq.1 [46]. It is this proposal that we develop here. In Section 2 we review the data, both those used in [46] and many additional datasets. We show that the analyses of the datasets taken individually provide no support for Eq.1 and that these analyses can neither determine the value of x in Eq.4 nor even show that Eq.4 applies. In Section 3 we give a fully Bayesian analysis of the support the data taken as a whole (i.e. a meta-analysis) gives to the different hypotheses, Eq.1 and Eq.3. Finally, in Section 4 we compare the predictions of the different theories of the Hall-Petch effect with the data. We conclude that Eq.3 and the theory from which it derives always apply. That is, it describes the size dependence of dislocation plasticity *in general*, and *specifically* in the grain-size effect, while of course underlying other effects which may also increase the strength of metals. The indelible may yet be erased.

2. Review and analysis of the data

We present in Fig.1 sixty-one datasets of which seventeen were already considered in [46]. These data sets, among many others, are what is referred to by the authors cited above who say that the data supports Eq.1. We show in Section 2.2 that these datasets support neither Eq.1 nor even Eq.4. In Section 3, we use meta-analysis to show that the ensemble of data supports Eq.3 very strongly.

2.1. *Data selection and presentation*

The data presented here have not been selected in any way. They are simply all the data we have found at the time of writing relevant to testing Eq.1. Our literature search methods consist of using information from colleagues, following up references and citations and internet search engine results. It is highly implausible that these methods would yield a selective sampling of the literature that could be biased against data supporting Eq.1.

Most of the original authors plotted against the inverse square-root of grain size and reported straight-line fits in accordance with Eq.1. Digitised and changed from the authors' units to SI units, all the full datasets are given in the supplementary electronic information. Normalised by Young's modulus Y and lattice constant a_0, they are plotted in Fig.1, on double logarithmic axes because of the very wide range of data values. It is worth noting here that the exact value of Y for each metal is not important. The purpose is

to facilitate comparisons by taking out the *known* differences between metals. We use average or representative values from handbooks for each metal, given below. Similarly, while the Burgers vector **b** for each metal might be known quite accurately, the relevant projection *b* may not be, so we use the handbook values of lattice constant as a proxy. The fits shown in Fig.1 are described in Section 2.2. The heavy lines are Eq.3 drawn for $k = 0.72$ and $\varepsilon_0 = 0$. Two key features of these plots, analysed below, are that the different fits for $x = ½$ and $x = 1$ diverge significantly only outside the range of each dataset (Section 2.2), and that no data are found significantly below the Eq.3 $\varepsilon_0 = 0$ line (Section 3).

For each dataset, we give in the electronic supplementary information the information in the original papers about the metallurgical processing, especially grain-size modification and determination, and the yield or flow stress determination, or we mention the absence of this information. However, we do not use this information. The original authors did not correct their raw data for any known effects that might follow from these variables, and it would not appropriate, even if possible, to do so here.

The normalisation constants used for iron and steel are $Y = 211$ GPa, $a_0 = 0.287$ nm [46]. The data shown in Fig.1a come from Hall [1, 46] (the attribution to Ref.46 indicating that we used this data in [46], Fe(7); Petch [2, 46], Fe(1); Armstrong *et al.* [47], Fe(6) – here and below, where there are multiple datasets under one key it is because the authors reported data at various values of strain; Douthwaite [48], Fe(5); Douthwaite and Evans [49], Fe(2); Kashyap and Tangri (1997), Fe(4); Aghaie-Khafri *et al*. [23], Fe(3).

For brass and copper, we used $Y = 115$ GPa and $a_0 = 0.361$ nm [46]. Data shown in Fig.1b comes from Bassett and Davis [51, 46], B(1), B(2), and Babyak and Rhines [52,46]. We took this data from Jindal and Armstrong [53] who plotted this data against $d^{-½}$. Armstrong and Elban [54] also reported that Mathewson [22] fitted the inverse fourth-root to the data of Bassett and Davis [51]. Data comes also from [47, 46], B(4), and [48,46], B(5). The copper data in Fig.1c is from Feltham and Meakin [55], Cu3; Hansen and Ralph [56], Cu(1) (room temperature data) and Cu(2) (77K data).

Some of the data in Fig 1d is diamond point hardness (DPH) data, for which we divide by the Tabor factor of 2.8. For W (DPH) it comes from Vashi *et al*. [57, 46]; Cr (DPH) from Brittain *et al*. [58, 46]; Ti(1) (DPH), Hu and Cline [59, 46]; Jones and Conrad [60], Ti(2). For W we used $Y = 411$ GPa and $a_0 = 0.316$ nm; for Cr, $Y = 279$ GPa and $a_0 = 0.228$ nm; for Ti $Y = 116$ GPa and $a_0 = 0.295$ nm [46].
For silver, we used $Y = 83$ GPa and $a_0 = 0.409$ nm. The data in Fig.1e is from Aldrich and Armstrong [62], Ag(1), Ag(2). They compared linear fits to d^{-1}, $d^{-½}$ and $d^{-⅓}$ and concluded that $d^{-½}$ fitted best. They ruled out the $d^{-⅓}$ fit on the grounds that it gives an unphysical negative intercept on the y-axis – note that the datasets Fe(3), Au, Al(4) and Al(5) do the same in the $d^{-½}$ fits. The dataset Au, using $Y = 79$ GPa and $a_0 = 0.408$ nm is from Emery and Povirk [62]. The nickel data, with $Y = 200$ GPa and $a_0 = 0.352$ nm, is from Thompson [63], Ni(1); Keller and Hug [64], Ni(2); Narutani and Takamura [29], Ni(3). Keller and Hug studied foils with a thickness to grain size ratio t/d between 1.3 and 15. At yield stress, they observed a normal Hall-Petch behaviour for t/d =15 and we use this data. For higher strain and smaller t/d, deviations from the normal Hall-Petch behaviour were observed, and explained in terms of the effect of the free surface on the work-hardening mechanisms. This data is not considered here.

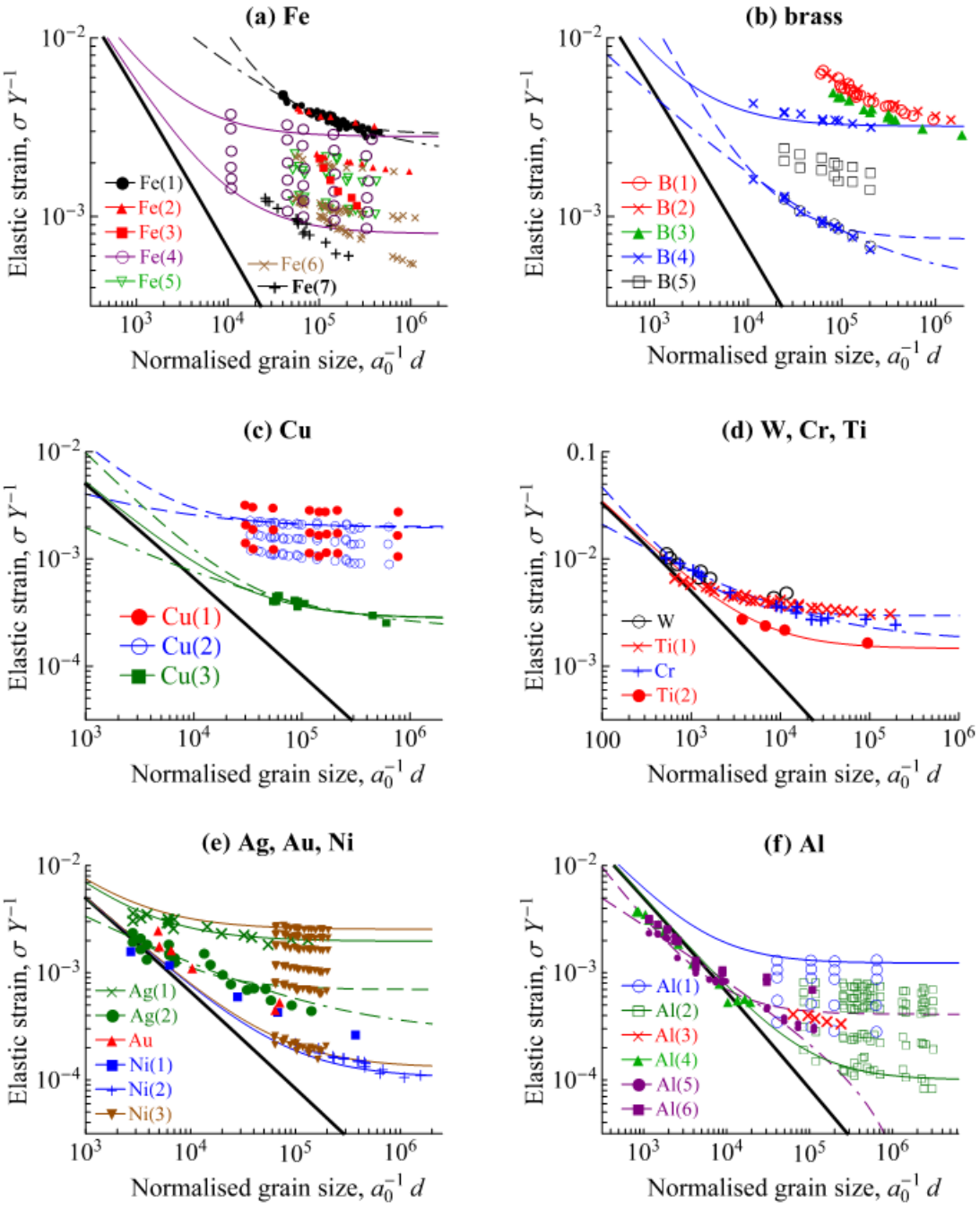

Fig.1. Normalised datasets from the literature for flow or yield stress against grain size. The heavy line in all panels is for Eq.3 with $k = 0.72$ and $\varepsilon_{0} = 0$. The dashed lines are fits using Eq.4 with $x = 1$, k and ε_0 as fitting parameters. The chain-dotted lines are fits using Eq.1, normalised, so that k_{HP} and ε_0 are the fitting parameters. The thin solid lines are for Eq.3 with $k = 0.72$ and ε_0 as the only fitting parameter. The keys link the datasets to the references cited in the text.

Fig.1f shows data for aluminium, using Y = 70 GPa and a_0 = 0.316 nm. They are from Carreker and Hibbard [65], Al(3); Hansen [66], Al(1) and Al(2); Tsuji *et al.* [67], Al(4); Yu *et al.* [68], Al(5) and Al(6).

2.2. *Fits to the data.*

Using the *Mathematica*© function *NonlinearModelFit* the data were fitted with Eq.1 (HP fit), with Eq.3 with k as a free fitting parameter (ECD fit), and with Eq.4 with x = 1 (SI fit) and also with x a free fitting parameter (EQ4 fit). Some (not all, for clarity) of these fits are shown in Fig.1. Full details, fitting parameter values and R^2 values are given in the supplementary electronic material.

All the fits are very good, with R^2 values typically well over 0.999. However, the exponents returned by the EQ4 fit are scattered about x = ½ – twenty-five are more than and twenty-five less than ½. All forty of the datasets returning x < 0.7 have R^2 values favouring the HP fit over the SI and ECD fits; only fifteen with x > 0.7 have R^2 values favouring the SI or EDC fits. These observations might be taken to favour the HP fit. A detailed analysis of a few typical datasets, however, shows that it is not so.

We choose Cu(1) for this detailed analysis because the three datasets in it have relatively little scatter, Ag(1) because it was considered by Aldrich and Armstrong [61] as potentially fitting exponents of x = 1/3, x = 1/2 and x = 1, and B(1) because, like many of the iron and steel datasets of Fig.1a, it has unusually high values of k_{HP} and k, and a wide range of grain size. Additional fits were carried out, to models with different functional forms, namely,

$$\text{LIN}: \quad \sigma = \sigma_0 - cd \qquad \text{A3}: \quad \sigma = \sigma_0 + \frac{k_{HP}}{d^{1/3}}$$

$$\text{EXP}: \quad \sigma = \sigma_0 + ce^{-\alpha d} \qquad \text{LOG}: \quad \sigma = \sigma_0 - c\ln d$$

The fits to LIN are to provide statistical benchmarks for a function that is surely not correct, and A3 because it was applied by Aldrich and Armstrong [61] to dataset Ag(1). The EXP and LOG fits are included to compare non-power-law fits with the power-law fits. Results of all eight fits are given in Table I. The LIN fit has the lowest R^2 coefficient of determination. The other seven, from SI through to EQ4, return $1 - R^2$ values (the proportion of the variance in the data which is *not* explained by the model) which are very small, and very similar for the different models across each dataset. The $1 - R^2$ values clearly reveal no evidence that the true dependence is a power-law dependence as in Eq.4, rather than any other function that is monotonically decreasing with grain size, asymptotically to σ_0 and so with some positive curvature, such as LOG and EXP. The silver data has more scatter than the other datasets, and therefore consistently higher values of $1 - R^2$. The only significant feature of these fits is that the model EQ4 returns consistently low values for the exponent x – though with large uncertainties – and consequently, generally better R^2 values even than the HP model.

Table I. Results of fitting real data and dummy datasets to eight models. All data are $(1 - R^2)$ values in ‰ (*per mill*, to reduce the number of zeroes) except the last column which gives the exponents returned by EQ4, x for the real datasets and $\bar{x}$ for the dummy datasets.

	LIN	SI	HP	A3	EDC	EXP	LOG	EQ4	$x,\ \bar{x}$
Cu(1) 5%	2.1	0.9	0.5	0.5	0.8	0.6	0.6	0.5	0.30 ± 0.16
Cu(1) 10%	1.1	0.7	0.6	0.6	0.7	0.6	0.6	0.6	0.22 ± 0.27
Cu(1) 20%	0.9	0.6	0.5	0.5	0.6	0.6	0.6	0.5	0.35 ± 0.39
Ag(1)	68	30	21	20	27	22	22	20	0.28 ± 0.19
B(1)	11	1.4	1.4	1.8	1.3	1.5	3.2	1.1	0.74 ± 0.13
HP*y*Cu	1.8	0.6	0.4	0.4	0.5	0.4	0.5	0.4	0.50 ± 0.16
HP*y*Ag	63	17	20	22	17	21	30	17	0.48 ± 0.18
SI*y*Cu	4.5	0.7	1.1	1.3	0.7	0.6	2.2	0.6	1.02 ± 0.21
SI*y*Ag	64	18	13	14	16	14	19	13	1.01 ± 0.25
HP*x*Cu	1.9	0.6	0.3	0.3	0.5	0.4	0.5	0.3	0.23 ± 0.15
HP*x*Ag	67	33	19	17	29	17	20	17	0.38 ± 0.11
SI*x*Cu	2.5	2.0	1.4	1.3	1.9	1.2	1.3	1.3	0.32 ± 0.20
SI*x*Ag	78	34	25	26	31	20	33	25	0.55 ± 0.18

There are, however, assumptions in the least-squares fitting procedures. The assumptions are that the grain sizes are as specified, that the scatter comes from Gaussian-distributed errors in the measurements of the yield or flow stresses, and that the least sum of squared residuals is an unbiased estimator. The effect of these assumptions is best demonstrated by setting up dummy datasets and subjecting them to the same fitting routines. First, the dummy datasets HP*y*Cu and HP*y*Ag, with random errors added to the *y* (stress) values,

$$(d_i, \sigma_i) = \left(d_i, \sigma_0 + \frac{k_{HP}}{\sqrt{d_i}} + \varepsilon_i \right) \tag{5}$$

where the d_i and the other parameters are taken from the Cu(1) 5% strain and the silver Ag(1) datasets and their HP fits. The random numbers ε_i are drawn from the normal distribution with mean $\mu = 0$, standard deviation $\sigma = 2.8$ MPa (equal to the standard deviation of the residuals in the HP fit to the Cu(1) 5% strain data) and $\sigma = 16$MPa for silver. Generating five hundred such datasets and fitting each with EQ4, exponents *x* are obtained with mean values $\bar{x}$ and standard deviations given in Table I. Similarly, dummy datasets SI*y*Cu and SI*y*Ag are set up according to Eq.5 but with the SI fits (k/d). From Table I, for these four dummy datasets, set up according to the assumptions above, and specifically with the random error in the data attributed entirely to σ (*y*-axis values), the fitting returns exponents the same within error as those used to create the dataset. (Note that the error in the mean is the standard deviation divided by $\sqrt{500}$). The R^2 values are comparable with those of the real datasets.

The situation is quite different when we put the scatter on the grain sizes instead of the stresses. Now the yield or flow stresses are taken to be definite. The errors in grain size measurement are expected to be proportional to grain size – i.e. a lognormal distribution – and so we set up dummy datasets as

$$(d_i, \sigma_i) = \left(\frac{k^2}{(\sigma_i - \sigma_0)^2} 10^{\varepsilon_i}, \sigma_i \right) \tag{6}$$

for HP and similarly for SI. The datasets are inverted (σ and d axes exchanged) and fitted with the inversions of the functions HP and SI to obtain the parameters k and σ_0. The random parameters ε_i are drawn from the normal distribution with mean $\mu = 0$, standard deviation 0.11 for copper and 0.18 for silver, chosen to give the same variance on the residuals as the HP fits. Fitting five hundred such datasets with the eight functions LIN to EQ4, R^2 values are much as before. But the exponents found by fitting with EQ4 are now dramatically smaller than the values used to set up the datasets, 0.2 – 0.4 for the HP dummy datasets where the true x = ½, and 0.3 – 0.6 for the SI datasets where the true x = 1.

2.3. *Discussion of fits to the data*

As noted in [46] for seventeen datasets and as confirmed quantitatively in Section 2.2 for sixty-one, fits of the data to Eq.1 and fits to Eqn.3 (with or without the ln$d$ term) are equally good. The rigorous statistical analysis given here confirms that the data cannot distinguish between these, nor between these and non-power-law models. From this analysis, there is no experimental support even for a power-law with uncertain or variable exponent x as in Eq.4. The most that can be said of the Hall-Petch effect from analysis of these datasets is that the strength decreases monotonically – but with positive curvature – as the grain size is increased.

The low values of the exponent obtained by fitting with Eq.4, and the low values reported in the literature for the last 60 years, are fully explained by assuming a moderate random error in the grain size determination. That is demonstrated here by using dummy datasets in standard non-linear least-squares fitting. An error analysis of the grain size determinations in the literature is not possible – Rhines [69] listed about ten ways of determining the grain size, and most authors do not give this detail. A deeper mathematical understanding of the effect of grain-size variance on the least-squares fitted exponent can be obtained by further analysis, but that is outside the scope of this paper. The vertical least-square residuals is a biased estimator for non-linear models, and Eq.4 is non-linear in x. So also will be the orthogonal least-square residuals estimator sometimes used, and especially relevant when fitting is done by eye, as much of the earlier data would have been. There exist fitting procedures that can handle errors in the independent variable (here, grain size), e.g. Deming regression, but they require estimates of the errors which are not available here.

Simulation and modelling are beginning to be able to display the Hall-Petch effect and predict Hall-Petch slopes (e.g. [42, 70, 71]). In this case, there is no error bar on the grain size, and such work is indeed beginning to show that Eq.3 is preferable to Eq.1 [43].

The outcome of this Section is to show that, without benefit of theory, the two and three-parameter fits, SI, HP, EDC and EQ4, cannot determine the true functional form obeyed by the data – not even to confirm it to be a power-law. In addition, an explanation is found, why Eq.1 might be considered to be the best fit to the data even if the data actually obeys Eq.3. In the next Section, we show that meta-analysis supported by theory can reach an unambiguous conclusion.

3. Bayesian meta-analysis of support for hypotheses

Previously [46], we reported an analysis of the statistical support that the data provides for the different theories, Eq.1 and Eq.3. We used the semi-Bayesian approach of calculating the likelihood L of the data under the two theories – which was inconclusive – and then using the Akaike information criterion (AIC), which provides a heavy weighting against theories with more free fitting parameters. Since the Hall-Petch theory of Eq.1 has two free fitting parameters per data set (σ_0 and k_{HP}; 34 parameters for 17 datasets) while the theory underlying Eq.3 has only one free fitting parameter per data set (σ_0) plus one ($k \sim 1$) for all datasets (18 parameters for 17 datasets), the AIC gave odds of many millions to one that the dislocation curvature theory is true and the Hall-Petch theory false.

Here we give a more fundamental, fully Bayesian analysis. Bayes' theorem may expressed in the form, the new odds on the hypothesis under test (H) being true when new data is acquired are the prior odds, times the ratio of the probability of the new data under the hypothesis H and its probability if H is false. Here, we may take H to be the hypothesis that Eq.3 is valid, and its negation $\sim H$ to be the hypothesis that Eq.1 is valid. This applies very directly to our problem. In the absence of a theory constraining the values of σ_0 and k_{HP} in Eq.1, the experimentally-determined values of yield or flow stress against grain size are expected to have a uniform probability distribution in the $\log\sigma_0$ – $\log d$ space, by Benford's Law [72, 73]. Let this probability distribution be represented by the relative value 1 everywhere. On the other hand, Eq.3 with $\sigma_0 = 0$ divides the $\log\sigma_0$ – $\log d$ space into two equal parts – one below the $1/d$ line (with or without the $\ln d$ term makes no significant difference) and one above. Eq.3 asserts that the probability that data will be significantly below the line is zero, so the data should be concentrated into the half of the space above the line. So, defining H as the hypothesis that Eq.3 is correct, we have a relative probability density of 2 for data above the $1/d$ line and 0 for data significantly below the $1/d$ line.

We apply Bayes' theorem iteratively for each dataset. We start by postulating a value for the the prior probability P_0 or odds O_0 that H is true before any data is considered. Using only the Principle of Insufficient Reason, we would take $P_0 = ½$, i.e. even odds, $O_0 = 1$ to 1. On the other hand, we might consider that the probability that an equation that has stood for sixty years is false is very low, so that perhaps we should take $P_0 = 10^{-3}$, $O_0 = 999$ to 1 against). The first dataset, that falls above the $1/d$ line, gives a value 2 to the second term on the RHS, so that the term on the LHS, the odds against H halve, or the odds on H double. This becomes the first term of the RHS (for $P_0 = ½$, $O_1 = 2$ to 1 on, $P_1 = ⅔$) when we consider the second dataset. As each successive dataset i falls above the $1/d$ line, $O_i = 2\ O_{i-1}$ and for n datasets $O_n = 2^n P_0$. So just ten or twenty such datasets give overwhelming odds on H, depending on whatever reasonable prior P_0 we may have chosen. Here we have 61 datasets, giving odds of $2^{61}P_0$ to one – which is overwhelming for any reasonable choice of prior P_0.

These odds on the Eq.3 hypothesis can be reduced slightly by considering that not all the datasets are independent. If the data for the yield point or lowest strain fall on and above the line, it is predictable that the data for the same material at higher strains at the same grain sizes will also fall above, so the observation that this is so does not strengthen the hypothesis. This reduces the number of fully-independent datasets to 32, which still leaves overwhelming odds on H.

The probability is not a step-function between 2 in the upper right and zero in the bottom left, below the Eq.3 line. If that were so, any data in the bottom left would immediately give a probability of zero for the hypothesis *H*. In fact, experimental error, grain-size determination, grain-size distributions and non-dislocation-based plasticity at small grain sizes all have a non-vanishing probability of putting data a little below the line. Thus the data seen there at ultra-fine grain sizes, Ni(1), Al(4), Al(5) and Al(6), may be accounted for by grain-boundary sliding, migration and diffusion which have been considered in connection with the inverse Hall-Petch effect (e.g. [74, 75]). The surprise, then, is how little data is there, not how much.

Finally since the conclusion of this Section is that Eq.3 (with $k \sim 1$ and variable ε_0 or σ_0) provides the best description of the data, we should consider the significant number of datasets in Fig.1 where the EDC-fitted value of *k* is much higher, Fe(1), Fe(3), B(1), B(2) and B(3). These datasets are as difficult to account for by the theories of Eq.1 (see Section 4) as by the theory of Eq.3. One speculation is suggested by the observation that these datasets are all for alloy metals, steels and brass. Microstructure in such metals has scope for size-effect lengths that may be much less than the grain size yet correlated with it. Alternatively, this may be a consequence of grain-size dependent strain-hardening as in [29].

4. One-parameter Hall-Petch theories

While experimentally Eq.1 is treated as if both σ_0 and k_{HP} are free fitting parameters, the theories which have been put forward to account for the inverse square-root law of Eq.1 do of course make predictions for k_{HP}. And the phenomena in question, when they occur in practice, must contribute to the strength. It is appropriate, therefore, to compare their predictions of k_{HP} with the data, to test whether they are in fact supported by the data and whether they explain the data. Classic theories of the Hall-Petch inverse-square-root dependence on *d* (Eq.1) are shown schematically in Fig.3(a-d) together with schematic representations of the dislocation curvature theory leading to Eq.3 in epitaxial layers (Fig.3e) and in polycrystalline metals (Fig.3f).

4.1. *Dislocation pile-up model*

This is the phenomenon most often used to account for the Hall-Petch Eq.1. In this model, a dislocation source in a grain operates many times under an applied stress to produce a number of dislocations on the same glide plane (Fig.3a). The leading dislocation experiences a force from the stress field, and also the forces from the following dislocations behind it, but it is blocked from further movement by the grain boundary. When the force on the leading dislocation is sufficient to stress the material at or beyond the grain boundary to theoretical strength (or some lower value), dislocations are produced in the neighbouring grain and large-scale plasticity becomes possible. Following Cottrell [76], Eshelby *et al.* [3] and Antolovich and Armstrong [77], the theory gives

$$\tau = \tau_0 + \sqrt{\frac{Gb\tau_C}{2\pi d}} \qquad (7)$$

where τ_c is the critical shear stress at the grain boundary at which a dislocation is generated in the neighbouring grain. The maximum reasonable value of τ_C is the

theoretical strength, less than $G/10$. For the use made of Eq.7 below (Fig.3a), differences between τ / G and σ / Y are unimportant, likewise the approximation $b \sim a_0$. Then Eq.7 becomes

$$\varepsilon_f - \varepsilon_0 \leq \frac{\sim 0.1}{\sqrt{a_0^{-1} d}} \tag{8}$$

for the elastic flow strain $\varepsilon_f = \sigma_f Y^{-1}$, in normalised units as used in Fig.1 and 3.

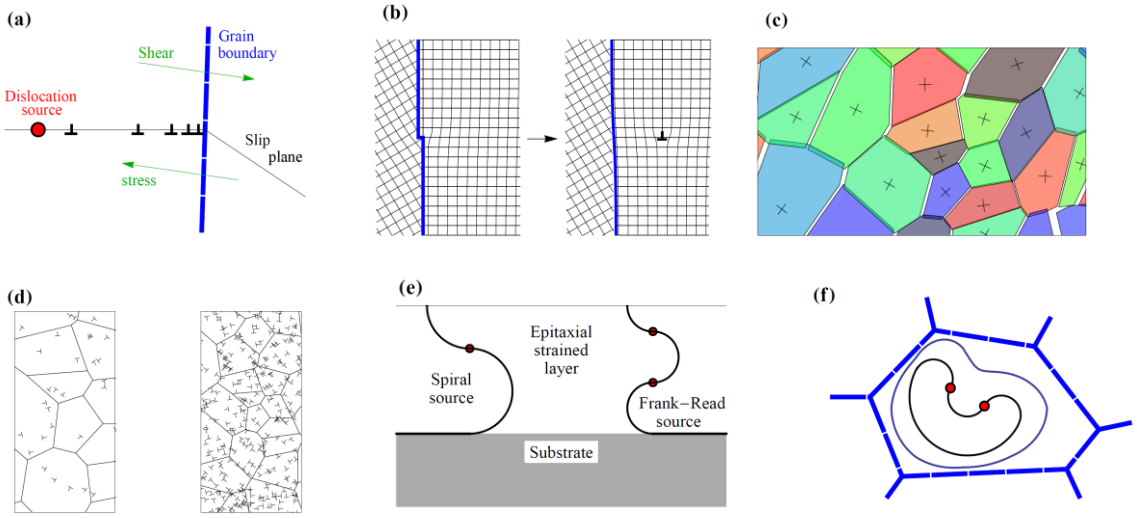

Fig.2. The four classic models are shown schematically (a–d) together with the dislocation curvature model (e, f). In (a), the pile-up theory of Eshelby *et al.* [3] is represented. The ledge-emission model of Li [78] is shown in (b). The effects of crystalline elastic or plastic anisotropy in forcing stress and strain gradients (Kelly [79], Meyers and Ashworth [80], Hirth [28], Ashby [81]) is illustrated in (c), in which anisotropic grains are subject to a homogenous stress field. In (d), the dislocation densities resulting from the slip-distance theory (Conrad [82], Kuhlmann-Wilsdorf [36]) are shown as low in large-grain and high in small-grain material. The Matthews critical thickness concept is illustrated in (e) for the form well-established in semiconductor epitaxy, for the spiral source and the Frank-Read source in a strained epitaxial layer on a substrate, and in (f) a Frank-Read source is shown in a single grain to illustrate that smaller grains require greater curvatures and hence stresses varying as $1/d$ or $\ln d / d$.

The data from Section 2 are compared with the prediction of the pile-up model in Fig.3a. The shaded triangle below the solid line is the allowed region according to Eq.9. Many of the datasets have slopes (values of k_{HP}) greater, even very much greater, than the predictions. Applying the same statistics as in Section 3, the odds *against* the pile-up model are greater than the odds *on* the hypothesis *H* that Eq.3 is correct; for many data are falling where their relative probability is much less than one-half. In fact this is an exaggeration. Different data sets falling where their probabilities are low may not be

independent events. Consider the *a priori* estimate of the (small) probability P_0 that the model is correct but the parameter values in Eq.7 have been wrongly estimated. Then all data wherever they fall are fully consistent with this hypothesis, which retains the probability P_0 independent of the data.

Pile-up can of course occur, and will give rise to some (grain-size dependent) strengthening. However, Fig.3a shows that it cannot account for the most part of the strength in most datasets; that is, it is a weak effect compared with the direct effect of grain size on the dislocation mechanisms that are required for plasticity (source operation, Eq.3). This conclusion is confirmed by discrete dislocation dynamics simulations of wires in torsion, in which pile-up can be encouraged by prohibiting cross-slip or reduced by allowing cross-slip. Torque-torsion curves did not change significantly with the amount of pile-up [83].

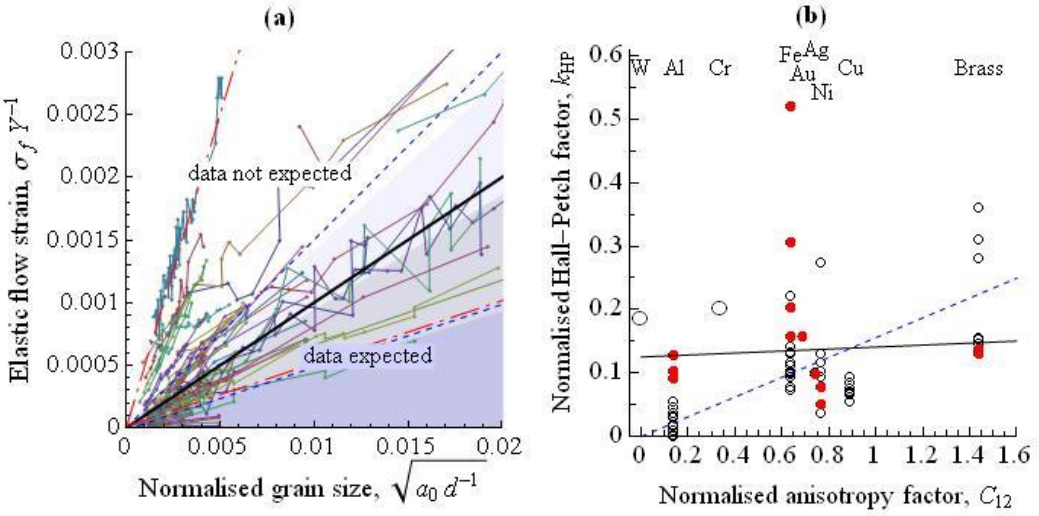

Fig.3. (a) The predictions of the pile-up model (Eq.8) (heavy black line), the grain-boundary ledge model (Eq.9) (dashed black lines indicating the range of the upper limit of the predictions) and the slip-distance model, Eq.13 (chain-dotted red lines) are compared with the data. The depth of shading indicates schematically the probability according to these models that data will fall in the various regions; white corresponds to a probability close to zero. In (b), the Hall-Petch coefficients are plotted against the normalised anisotropy factor as described in the text. The large data points indicate that only one data set is available for a metal; the small data points represent many results for the same metal. The red filled circles indicate the yield stress data sets. The latter are averaged to give a single value for each metal before fitting. The solid black line is a least-squares fit of $y = ax + b$ to the averaged data and the dashed blue line a fit of $y = ax$ as described in Section 4.4.

4.2. *Grain boundary ledge model*

Li [78] sought a model that could explain the Hall-Petch behaviour in the majority of cases where there is no evidence of dislocation pile-up. He proposed that grain boundaries and sub-grain boundaries should emit dislocations (Fig.2b). He showed that

the stresses required are nearly the same (1) for a pile-up to drive a dislocation through a grain boundary, (2) for a pile-up to activate a source on the other side of the boundary, and (3) to move dislocations in a forest formed by all the dislocations emitted by a tilt boundary. In model (3) the grain-size dependence arises from the density of the forest. Murr [84] reported observations by electron microscopy supporting this model. The prediction of the model is

$$\tau - \tau_0 = \alpha G b \sqrt{\frac{8m}{\pi d}} \tag{9}$$

where α is a constant of the order of 0.4, and the constant m is given by the expectation that the product mb will be in the range 0.02 to 0.2 [85-87]. Converting to $\varepsilon = \sigma/Y \sim \tau/G$ and using $b \sim a_0$, this becomes,

$$\varepsilon - \varepsilon_0 \sim \frac{0.05 - 0.15}{\sqrt{a_0^{-1} d}} \tag{10}$$

Fig.3a shows the range where data is to be expected according to Eq.10. This model is again inconsistent with much of the data, and it does not account for the wide scatter of the data. The same considerations apply to the probability that it is correct as for the pile-up model in Section 4.1.

4.3. *Plastic strain models*

There is a class of theories which give the Hall-Petch coefficient as dependent on plastic strain (with no Hall-Petch effect at the yield point). This is too large a topic to deal with adequately here, so we consider one typical theory. Conrad [82] and co-workers [88, 85] developed a theory which gives very naturally the inverse square-root dependence on grain size of Eq.1 when square-root strain-hardening occurs. See also [36, 29]. Mobile dislocations account for the plastic strain ε_{pl}, and

$$\varepsilon_{pl} = \rho_m b \bar{x} \tag{11}$$

where ρ_m is the density of mobile dislocation and $\bar{x}$ is their mean free path, taken as proportional to the grain size, $\bar{x} = \lambda d$ It is further assumed that a constant proportion of the total dislocation density ρ is mobile, so that $\rho_m = \xi\rho$. Using the Taylor (forest) hardening expression, substituting and rearranging, we have

$$\tau - \tau_0 = \alpha G b \sqrt{\rho} = \alpha G \sqrt{\frac{b\varepsilon_{pl}}{\lambda \xi d}} \tag{12}$$

where α is the Taylor coefficient. Converting as for Eq.10,

$$\varepsilon - \varepsilon_0 = \alpha \sqrt{\frac{\varepsilon_{pl}}{\lambda \xi}} \sqrt{a_0 d^{-1}} \tag{13}$$

Thus the model attributes the Hall-Petch effect to the increased dislocation density in small grains (Fig.2c) due to the reduced slip distance. This gives a Hall-Petch coefficient which vanishes at the yield point ($\varepsilon_{pl} = 0$) and is proportional to the square-root of plastic strain otherwise. The constant α is normally taken as about 0.3, while the constants λ and ξ are both of the order of but less than unity, so the factor $\alpha^2 / \lambda\xi$ may be taken to be about unity. Then for the datasets reported at high plastic strains ~0.2, the value of k_{HP} in Eq.13 may be close to 0.5, while for the datasets reported near the yield point ($\varepsilon_{pl} \sim$

0.002) it will be below 0.05. These two possibilities are plotted on Fig.3a (red chain-dotted lines). Clearly, this theory can be ruled out for the Hall-Petch effect near the yield point, but it survives as a candidate for explaining Eq.1 behaviour at high plastic strains when square-root strain-hardening is observed.

Other theories, such as the plastic anisotropy theory of Ashby [81], give very similar expressions for k_{HP}, so the same comments apply. However, before leaving the topic for a fuller treatment elsewhere, it is worth noting that the datasets Fe(4), Fe(5), Fe(6), B(4), B(5), Cu(1), Cu(2), Ag(1,2) Al(1) and Al(2) all have data for different strains. Any dependence of k_{HP} on the plastic strain is weak or absent. Only Ni(3), from Narutani and Takamura [29], shows the strong dependence expected from these theories – and these authors note that their data deviates from Eq.1.

4.4. *Elastic anisotropy model*

This model was proposed by Kelly [79], Hirth [28] and Meyers and Ashworth [80]. Given the random orientation of grains, a homogenous elastic stress field necessitates an inhomogeneous elastic strain field, resulting in gaps and overlaps between grains as shown in Fig.3d. Here a two-dimensional polycrystalline cubic material with non-zero anisotropy $C = |c_{11} - c_{12} - 2c_{44}|$ is shown elastically deformed under a uniform shear stress field. Gaps and overlaps form. Deforming the grains to eliminate them results in inhomogeneous stress and strain fields. The resulting strain gradients require the creation of geometrically necessary dislocations if plastic deformation is to occur, and a consequent increase in strength. The grain-size dependence arises naturally, in that if the grains are smaller the strain gradients and the densities of GNDs will be proportionately larger. This model predicts that under suitable normalisation k_{HP} will be proportional to the elastic anisotropy. The factor of proportionality is unspecified by the theory – it is phenomenological, depending on the characteristic length in the strain-gradient theory, which can only be found by experiment. In Fig.3b we plot the values of k_{HP} for the cubic metals against their normalised anisotropy parameters C/Y . While there is a considerable scatter of the data for metals where we have more than one value of k_{HP}, it is clear that there is no strict dependence, nor even a trend suggesting that k_{HP} depends upon C. This model is therefore neither consistent with nor explanatory of the data.

4.5. *Discussion*

The outcome of this Section is that none of these theories explain the observed strength of metals as a function of grain size. They fail in a variety of ways, including unfulfilled predictions of parameter values and of functional dependence on known parameters, but most fundamentally they fail against the Bayesian criticism – none of them are consistent with all the data appearing above the Eq.3 ($\sigma_0 = 0$) line of Fig.1 and almost no data below. The odds against them are thus consistently millions to one against.

5. Conclusions

It is clear that there is neither experimental nor theoretical evidence for the 60-year-old Hall-Petch equation, Eq.1. The role of errors in grain-size determination in approximately halving the apparent exponent in least-squares fitting has previously been overlooked, but is a very plausible explanation for the apparent agreement of the data

with the Eq.1 value of $x = ½$ if the data actually obey $\ln d/d$ or d^{-1}. The wide range of experimentally reported values for the Hall-Petch constant, k_{HP}, for similar materials do not support Eq. 1, neither are they predicted by any of the theories in section 4. On the other hand, the large body of experimental data is fully consistent with the size-effect expected from dislocation curvature, Eq.3, for the minimum strength expected for a given grain size. That consistency depends on the necessary caveats: non-dislocation based plasticity such as grain-boundary sliding may take over at small grain sizes; other strengthening mechanisms may be correlated with grain size with or without being caused by grain size.

An argument in favour of this conclusion is that it brings the Hall-Petch effect under the umbrella of the size effect(s) generally, rather than being *sui generis* with its own unique inverse-square-root exponent and therefore a need for its own explanations. We argue that the underlying size-dependence that dictates the minimum strength for dislocation plasticity should be in the singular – the only size effect that will be necessarily present in all experimental situations is the Orowan size-stress relationship, *aka* Matthews critical thickness theory [5], *aka* the argument from similitude [37]: the size must be inversely proportional to dislocation curvature and hence to stress.

It might be considered that this doesn't matter. It might be pointed out that the Hall-Petch relation, Eq.1, is a valid empirical relation and as such it is useful for prediction – for interpolation and extrapolation of material properties – whether or not it is theoretically correct [28]. That is certainly so for interpolation, for which it will be as useful – but no more useful – than a smooth curve drawn through the data by hand – but this is a very dangerous approach to extrapolation.

One may also regret the loss of time – the wasted effort – in attempts to explain the inverse-square-root form of Eq.1, and of course the parameter values therein too. On the other hand, one may anticipate theoretical and practical advances that may be made when it is considered that the grain-size effect operates through the same mechanism as other size effects and therefore may be combined with them, as in Ehrler coupling of structural size and grain size [89].

The other main conclusion from this work is that it can never be sufficiently strongly emphasised that a good fit of data to an equation or to a theory is of no significance unless it has been adequately considered what else might fit the data. And statistical methods such as least-squares fitting should always be tested with dummy data where one knows what outputs should be obtained. This is a much more general conclusion, of interest to non-metallurgists as much as to metallurgists.

Ethics Statement: Not relevant.
Data accessibility: All sixty-one datasets used are given in full in the supplementary material.
Competing interests: We have no competing interests.
Authors' contributions: YL carried out the data digitization and data analysis, and drafted the manuscript; AJB and DJD jointly conceived of the study, designed the study, coordinated the study and finalised the manuscript. All authors gave final approval for publication.
Acknowledgements: Too many colleagues have contributed valuable insights and comments to name them all. But one must be singled out. We are very grateful to Prof.

Ron Armstrong, who appears frequently in the list of references, for his assistance in accessing the older literature, and especially for his encouragement and his enthusiasm for a re-appraisal of a topic with which he has been intimately concerned for well over fifty years.
Funding: YL is grateful to the Chinese Scholarship Council for his PhD studentship. AJB and DJD acknowledge the EPSRC grant EP/C518004 under which this work was initiated.

References

1. Hall, E.O., 1951. The deformation and ageing of mild steel: III Discussion of results. Proc. Phys. Soc. B 64, 747–753.
2. Petch, N.J., 1953. The cleavage strength of polycrystals. J. Iron Steel Institute 174, 25–28.
3. Eshelby, J.D., Frank, F.C., Nabarro, F.R.N., 1951. The equilibrium of linear arrays of dislocations. Phil Mag. 42, 351–364.
4. Frank, F.C., van der Merwe, J.H., 1949. One-dimensional dislocations. II. Misfitting monolayers and oriented overgrowth. Proc. Roy. Soc. A198, 216–225.
5. Matthews, J.W., Mader, S., Light, T.B., 1970. Accommodation of misfit across the interface between crystals of semiconducting compounds or elements. J. Appl. Phys. 41, 3800–3804.
6. Dunstan, D.J., 1997. Strain and strain relaxation in semiconductors. J. Mater. Sci.: Mater. in Electronics **8**, 337–375.
7. Adams, A.R., 2011. Strained-layer quantum-well lasers. IEEE J. Selected Topics Quantum Electronics 17, 1364–1373.
8. O'Reilly, E.P., 1989. Valence band engineering in strained-layer structures. Semicon. Sci. Technol. 4, 121–137.
9. Beanland, R., 1992. Multiplication of misfit dislocations in epitaxial layers. J. Appl Phys. 72, 4031–4035.
10. Beanland, R, 1995. Dislocation multiplication mechanisms in low-misfit strained epitaxial layers. J. Appl Phys. 77, 6217–6222.
11. Dunstan, D.J., Kidd, P., Beanland, R., Sacedón, A., Calleja, A., González, L., González, Y., Pacheco, F.J. 1996. Predictability of plastic relaxation in metamorphic epitaxy. Mater. Sci. Technol. 12, 181–186.
12. Nix, W.D., Gao, H., 1998. Indentation size effects in crystalline materials: A law for strain gradient plasticity. J. Mech. Phys. Sol. 46, 411–425.
13. Fleck, N.A., Muller, G.M., Ashby, M.F., Hutchinson, J.W., 1994. Strain gradient plasticity: Theory and experiment. Acta Metal. Mater. 42, 475–487.
14. Stölken J.S., Evans, A.G.., 1998. A microbend test method for measuring the plasticity length scale. Acta Met. 46, 5109–5115.
15. Uchic, M.D., Dimiduk, D.M., Florando, J.N., Nix, W.D., 2004. Sample dimensions influence strength and crystal plasticity. Science 305, 986–989.
16. Nix, W.D., 1989. Mechanical properties of thin films. Metall. Trans. 20A, 2217–2245.
17. Thompson, C.V., 1993. The yield stress of polycrystalline thin films. J. Mater. Res. 8, 237–238.

18. Dunstan, D.J., Bushby, A.J., 2004. Theory of deformation in small volumes of materials. Proc. Roy. Soc. A460, 2781–2796.
19. Korte, S., Clegg, W.J., 2010. Discussion of the dependence of the effect of size on the yield stress in hard materials studied by microcompression of MgO. Phil. Mag. 91, 1150–1162.
20. Kraft, O., Gruber, P.A., Mönig, R., Weygand, D., 2010. Plasticity in confined dimensions. Annual Review of Material Research 40, 293–317.
21. Dunstan, D.J., Bushby, A.J., 2013. The scaling exponent in the size effect of small scale plastic deformation. Int. J. Plasticity 40, 152–162.
22. Mathewson, C.H., 1919. Discussion. Trans. TMS-AIME 60, 451–455.
23. Aghaie-Khafri, M., Honarvar, F., Zanganeh, S., 2012. Characterisation of grain size and yield strength in AISI 301 stainless steel using ultrasonic attenuation measurements. J. Nondestruct. Eval. 31, 191–196.
24. Baldwin, W.M., 1958. Yield strength of metals as a function of grain size. Acta Metall. 6, 139–141.
25. Kocks, U.F., 1959. Comments on "Yield strength of metals as a function of grain size". Acta Metall. 7, 131.
26. Kocks, U.F., 1970. The relationship between polycrystal deformation and single-crystal deformation. Met. Trans. 1, 1121–1143.
27. Bragg, L., 1942. A theory of the strength of metals. Nature 149, 511–513.
28. Hirth, J.P. 1972. The influence of grain boundaries on mechanical properties. Met. Trans. 3, 3047–3067.
29. Narutani, T., Takamura, J., 1991. Grain-size strengthening in terms of dislocation density measured by resistivity. Acta Met. Mat. 39, 2037–2049.
30. Arzt, E., 1998. Size effects in materials due to microstructural and dimensional constraints: A comparative review. Acta Mat. 46, 5611–5626.
31. Saada, G., 2005. Hall-Petch revisited. Mat. Sci. Eng. A400-401, 146-149.
32. Holt, D.L., 1970. Dislocation cell formation in metals. J. Appl. Phys. 41, 3197–3201.
33. Thompson, A.W., 1970. Substructure strengthening mechanisms. Metall. Trans. 8A 833–842.
34. Raj, S.V., Pharr, G.M., 1986. A compilation and analysis for the stress dependence of the subgrain size. Mater. Sci. Eng. 81, 217–237.
35. Langford, G., Cohen, M., 1970. Calculation of cell-size strengthening of wire-drawn iron. Met. Trans. 1, 1478–1480.
36. Kuhlmann-Wilsdorf, D., 1970. A critical test on theories of work-hardening for the case of drawn iron wire. Metall. Trans. 1, 3173–3179.
37. Kuhlmann-Wilsdorf, D., van der Merwe, J.H., 1982. Theory of dislocation cell sizes in deformed metals. Mater. Sci. Eng. 55, 79–83.
38. Kuhlmann-Wilsdorf, D., Hansen, N., 1991. Geometrically necessary, incidental and subgrain boundaries. Scripta Met. Mat. 25, 1557–1562.
39. Yelon, A., Sacher E., Linert, W., 2012. Comment on "The mathematical origins of the kinetic compensation effect Parts 1 and 2" by P. J. Barrie, Phys. Chem. Chem. Phys., 2012, 14, 318 and 327. Phys. Chem. Chem. Phys. 14, 8232–8234.
40. Dunstan, D.J., 1998. The role of experimental error in Arrhenius plots: Self-diffusion in semiconductors. Solid State Commun. 107, 159–163.

41. Ohno, N., Okumura, D., 2007. Higher-order stress and grain size effects due to self-energy of geometrically necessary dislocations. J. Mech. Phys. Solids 55, 1879–1898.
42. Balint, D.S., Deshpande, V.S., Needleman, A., Van der Giessen, E., 2008. Discrete dislocation plasticity analysis of the grain size dependence of the flow strength of polycrystals. Int. J. Plasticity 24, 2149–2172.
43. Tarleton, E., Balint, D.S., Gong, J., Wilkinson, A.J., 2015. A discrete dislocation plasticity study of the micro-cantilever size effect. Acta Mat. 88, 271–282.
44. Hahn, E.N., Meyers, M.A., 2015. Grain-size dependent behaviour of nanocrystalline metals. Mat. Sci & Eng. A646, 101–134.
45. Hansen, N., 2004. Hall-Petch relation and boundary strengthening. Scripta Mat. 51, 801–806.
46. Dunstan, D.J., Bushby, A.J., 2014. Grain size dependence of the strength of metals: The Hall–Petch effect does not scale as the inverse square root of grain size. Int. J. Plasticity 53, 56–65.
47. Armstrong, R., Codd, I., Douthwaite, R.M., Petch, N.J., 1962. The plastic deformation of polycrystalline aggregates. Phil. Mag 7, 45–58.
48. Douthwaite, R.M., 1970. Relationship between the hardness, flow stress, and grain size of metals. J. Iron Steel Institute 208, 265–269.
49. Douthwaite, R.M. and Evans, J.T., 1973. Microstrain in polycrystalline aggregates. Acta Met. 21, 525–530.
50. Kashyap, B.P., Tangri, K., 1997. Hall-Petch relationship and substructural evolution in boron containing type 316L stainless steel. Acta Mat. 45, 2383–2395.
51. Bassett, W.H., Davis, C.H., 1919. Comparison of grain-size measurements and Brinell hardness of cartridge brass. Trans. TMS-AIME 60, 428–449.
52. Babyak, W.J., Rhines, F.N., 1960. The relationship between the boundary area and hardness of recrystallized cartridge brass. Trans. TMS-AIME 218, 21–23.
53. Jindal, P.C., Armstrong, R.W., 1967. The dependence of the hardness of cartridge brass on grain size. Trans. TMS-AIME 239, 1856–1857.
54. Armstrong, R.W., Elban, W.L., 2012. Hardness properties across multiscales of applied loads and material structures. Mater. Sci. Technol. 28, 1060–1071.
55. Feltham, P., Meakin, J.D., 1957. On the mechanism of work hardening in face-centred cubic metals, with special reference to polycrystalline copper. Phil. Mag. 2, 105–112.
56. Hansen, N., Ralph, B., 1982. The strain and grain size dependence of the flow stress of copper. Acta Met. 30, 411–417.
57. Vashi, U.K., Armstrong, R.W., Zima, G.E., 1970. The hardness and grain size of consolidated tungsten powder. Metall. Trans. 1, 1769–1771.
58. Brittain, C.P., Armstrong, R.W., Smith, G.C., 1985. Hall-Petch dependence for ultrafine grain size electrodeposited chromium. Scripta Metall. 19, 89–91.
59. Hu, H., Cline, R.S., 1968. Mechanism of reorientation during recrystallization of polycrystalline titanium. Trans. TMS-AIME. 242, 1013–1024.
60. Jones, R.L. and Conrad, H., 1969. Trans. TMS-AIME 245, 779. Data given in Abbaschian, R.and Reed-Hill, R.E., 2010. Physical Metallurgy Principles (Cengage Learning), p.192.
61. Aldrich, J.W., Armstrong, R.W., 1970. The grain size dependence of the yield, flow and fracture stress of commercial purity silver. Metall. Trans. 1, 2547–2550.

62. Emery, R.D., Povirk, G.L., 2003. Tensile behaviour of free-standing gold films. Part I: Coarse-grained films. Acta Mat. 51, 2067–2078.
63. Thompson, A.W., 1977. Effect of grain size on work hardening in nickel. Metallurgica 25, 83–86.
64. Keller, C., Hug, E., 2008. Hall-Petch behaviour of Ni polycrystals with a few grains per thickness. Mater. Lett. 62, 1718–1720.
65. Carreker, R.P., Hibbard, W.R., 1955, Wright Air Development Center Technical Report 55-113.
66. Hansen, N., 1977. The effect of grain size and strain on the tensile flow stress of aluminium at room temperature. Acta Metall. 25, 863–869.
67. Tsuji, N., Ito, Y., Saito, Y., Minamino, Y., 2002. Strength and ductility of ultrafine grained aluminum and iron produced by ARB and annealing. Scripta Mater. 47, 893–899.
68. Yu, C.Y., Kao, P.W., Chang, C.P., 2005. Transition of tensile deformation behaviors in ultrafine-grained aluminium. Acta Mat. 53, 4019–4028.
69. Rhines, F.N., 1970. Geometry of grain boundaries. Met. Trans. 1, 1105–1120.
70. Lim, H., Lee, M.G., Kim, J.H., Adams, B.L., Wagoner, R.H., 2011. Simulation of polycrystal deformation with grain and grain boundary effects. Int. J. Plasticity 27, 1328–1354.
71. Lim, H., Subedi, S., Fullwood, D.T., Adams, B.L., Wagoner, R.H., 2014. A practical mesoscale polycrystal model to predict dislocation densities and the Hall-Petch effect. Mater. Trans. 55, 35–38.
72. Newcomb, S., 1881. Note on the frequency of use of the different digits in natural numbers. Am. J. Math. 4, 39–40.
73. Benford, F., 1938. The law of anomalous numbers. Proc. Am. Philos. Soc. 78, 551–572.
74. Schiøtz, J., Vegge, T., Tolla, F.D.D., Jacobesen, K.W., 1999. Atomic-scale simulations of the mechanical deformation of nanocrystalline metals. Phys. Rev. B 60, 11971-11983.
75. Wolf, D., Yamakov, V., Phillpot, S.R., Mukherjee, A.K., 2003. Deformation mechanism and inverse Hall–Petch behavior in nanocrystalline materials. Zeitschrift für Metallkunde 94, 1091–1097.
76. Cottrell, A.H., Bilby B.A., 1949. Dislocation theory of yielding and strain ageing of iron. Proc. Phys. Soc. London A62, 49–62.
77. Antolovich, S.D., Armstrong, R.W., 2014. Plastic strain localization in metals: Origins and consequences. Prog. Mater. Sci. 59, 1–160.
78. Li, J.M.C., 1963. Petch relation and grain boundary sources. Trans. TMS 227, 239–247.
79. Kelly, A., 1966. Strong Solids (Clarendon Press, Oxford) p.84.
80. Meyers, M.A., Ashworth, E., 1982. A model for the effect of grain size on the yield stress of metals. Phil. Mag. A, 737–759.
81. Ashby, M.F., 1970. The deformation of plastically non-homogeneous materials. Phil. Mag. 21, 399–424.
82. Conrad, H., 1963. Effect of grain size on the lower yield and flow stress on iron and steel. Acta Met. 11, 75–77.

83. Senger, J., Weygand, D., Dunstan D.J., 2012. Private communication (unpublished); work presented at TMS 2013 and Plasticity 2014.
84. Murr, L.E., 1975. Some observations of grain boundary ledges and ledges as dislocation sources in metals and alloys. Met. Trans. 6A, 505–513.
85. Chia, K.-H, Jung, K., Conrad, H., 2005. Dislocation density model for the effect of grain size on the flow stress of a Ti–15.2 at% Mo β-alloy at 4.2–650 K. Mater. Sci. Eng. A409, 32–38.
86. Conrad, H., Jung, K., 2005. Effect of grain size from millimetres to nanometers on the flow stress and deformation kinetics of Ag. Mater. Sci. Eng. A391, 272–284.
87. Zhu, T.T., Bushby, A.J., Dunstan, D.J., 2008. Materials mechanical size effects: a review. Mater. Technol. 23, 193–209.
88. Conrad, H., Feuerstein, S., Rice, L., 1967. Effects of grain size on the dislocation density and flow stress of niobium. Mater. Sci. Eng. 2, 157–168.
89. Dunstan, D.J., Ehrler, B., Bossis, R., Joly, S., P'ng, K.M.Y., Bushby, A.J., 2009. Elastic limit and strain hardening of thin wires in torsion. Phys. Rev. Lett. 103, 155501.